

## **Supporting Information**

### **Wide-bandgap $\text{CaSnO}_3$ perovskite as an efficient and selective deep-UV absorber for self-powered and high-performance p-i-n photodetector**

*Manh Hoang Tran, Taehyun Park, Jaehyun Hur\**

Department of Chemical and Biological Engineering, Gachon University, Seongnam, Gyeonggi 13120, Republic of Korea

\*Corresponding author. Tel: +82-31-750-5593; Fax: +82-31-750-8839

E-mail address: [jhhur@gachon.ac.kr](mailto:jhhur@gachon.ac.kr)

## Contents

**Figure S1.** Particle-size distribution of  $\text{CaSnO}_3$  NPs.

**Figure S2.** SEM of the one-time spin-coated  $\text{CaSnO}_3$  layer.

**Figure S3.** I–V curves under dark of prepared p-n and p-i-n devices.

**Figure S4.** Statistics of photocurrent values for p-n,  $\text{pi}_1\text{n}$ ,  $\text{pi}_2\text{n}$ ,  $\text{pi}_3\text{n}$ ,  $\text{pi}_4\text{n}$ , and  $\text{pi}_5\text{n}$  devices.

**Figure S5.** UV-Vis spectra of the  $\text{SnO}_2$  and  $\text{CaSnO}_3$  films.

**Figure S6.** FIB-SEM image of the  $\text{CaSnO}_3$ -based p-i-n detector ( $\text{pi}_2\text{n}$  device).

**Figure S7.** Photoresponses of the p-n device under 254 nm and 365 nm UV illumination at 0 V.

**Figure S8.** Photocurrent density of  $\text{pi}_2\text{n}$  device and power density of light source with wavelength.

**Figure S9.** Photoresponse of  $\text{CaSnO}_3$ -based photodetector with PH1000/ $\text{CaSnO}_3$ /Ag structure.

**Figure S10.** Schematic illustration of p-i-n photodetectors preparation.

**Figure S11.** UV-Vis spectra of methanol-treated and untreated PH1000 film.

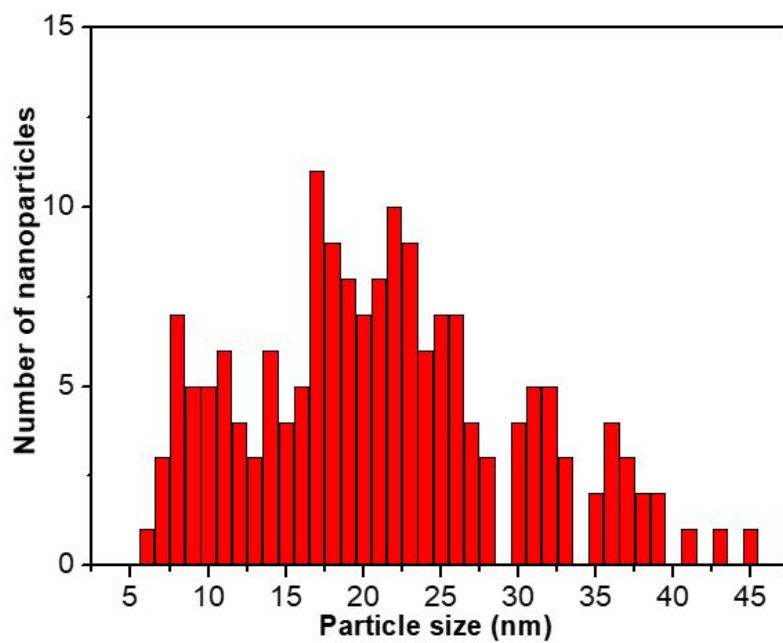


**Figure S1.** Particle-size distribution of CaSnO<sub>3</sub> NPs. Data was extracted from the TEM images using the ImageJ software (version 1.51, Bethesda, Maryland, USA).

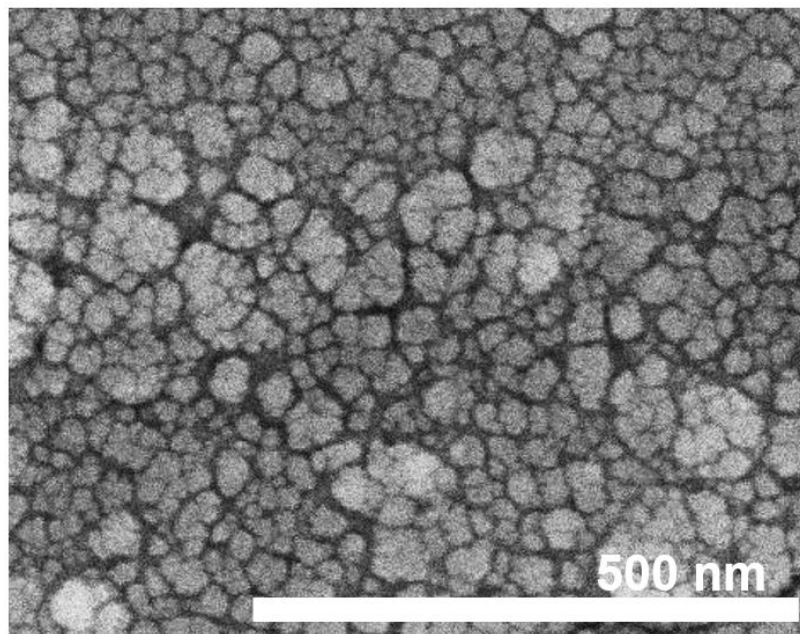


**Figure S2.** SEM of the one-time spin-coated  $\text{CaSnO}_3$  layer.

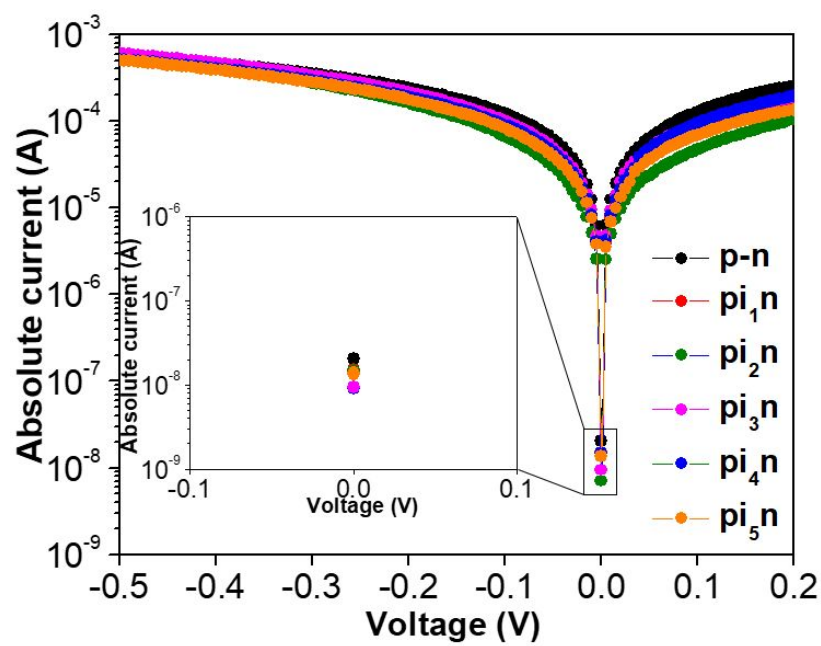


**Figure S3.** I–V curves of prepared p-n and p-i-n devices under dark conditions.

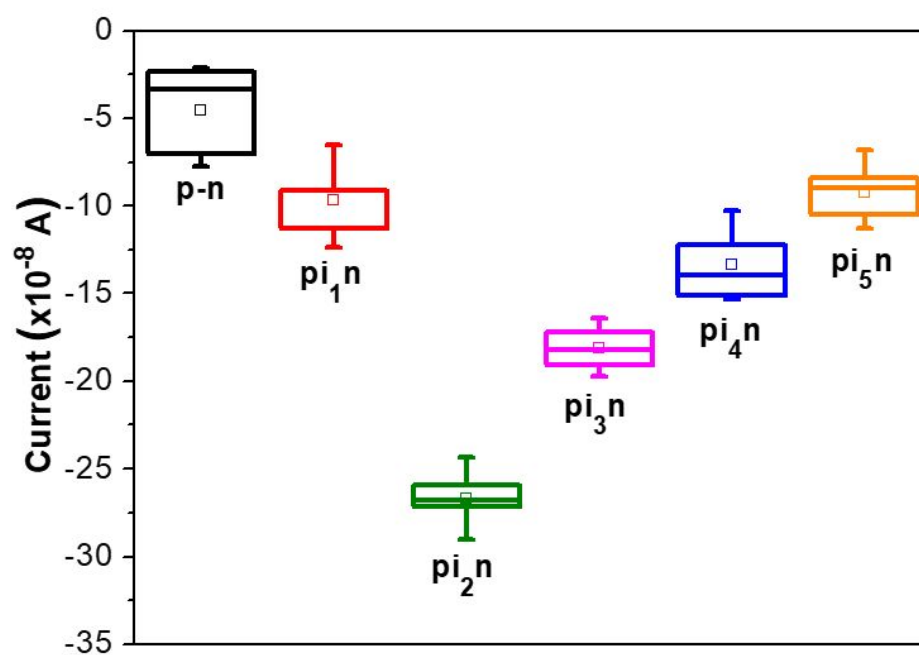


**Figure S4.** Statistics of photocurrent values for p-n,  $\pi_1n$ ,  $\pi_2n$ ,  $\pi_3n$ ,  $\pi_4n$ , and  $\pi_5n$  devices (each batch has five devices).

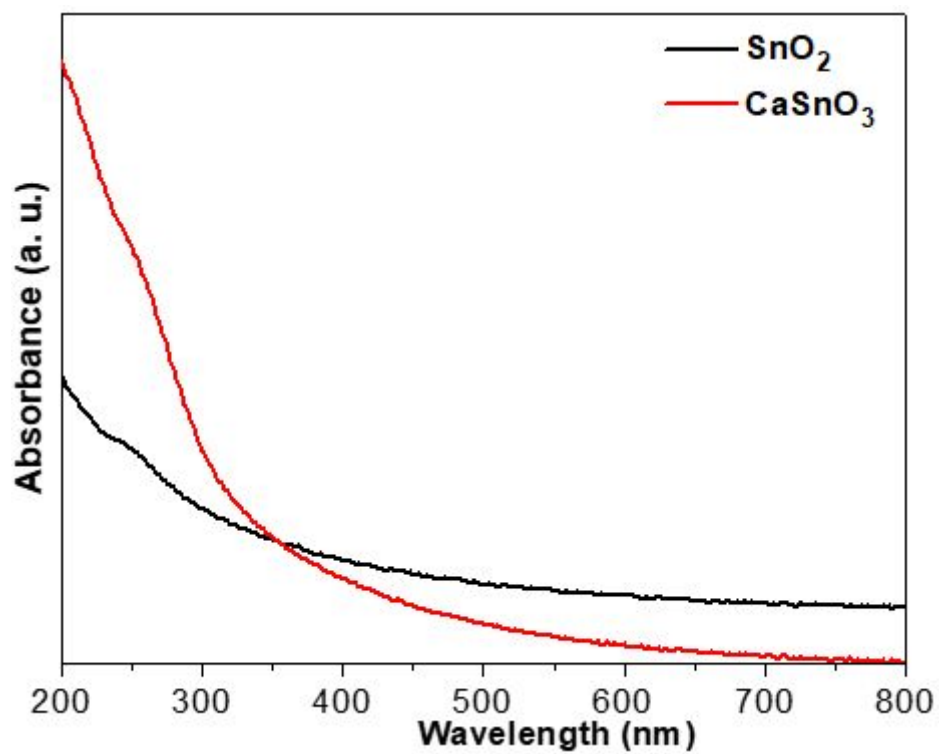


**Figure S5.** UV-Vis spectra of the two-time spin-coated SnO<sub>2</sub> and CaSnO<sub>3</sub> films.

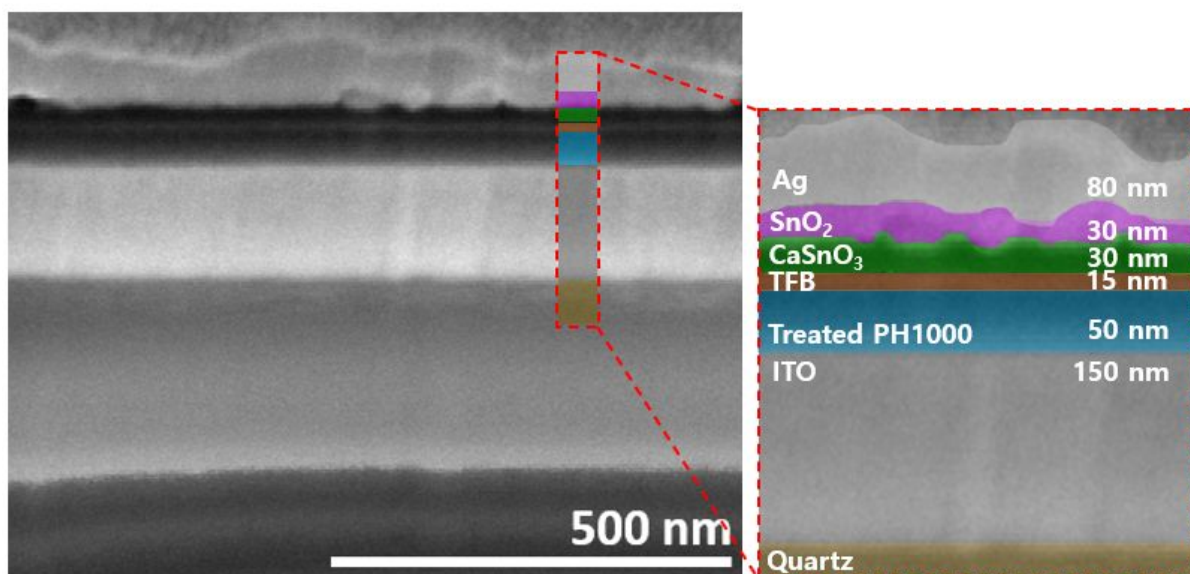


**Figure S6.** FIB-SEM image of the  $\text{CaSnO}_3$ -based p-i-n detector ( $\text{pi}_2\text{n}$  device).



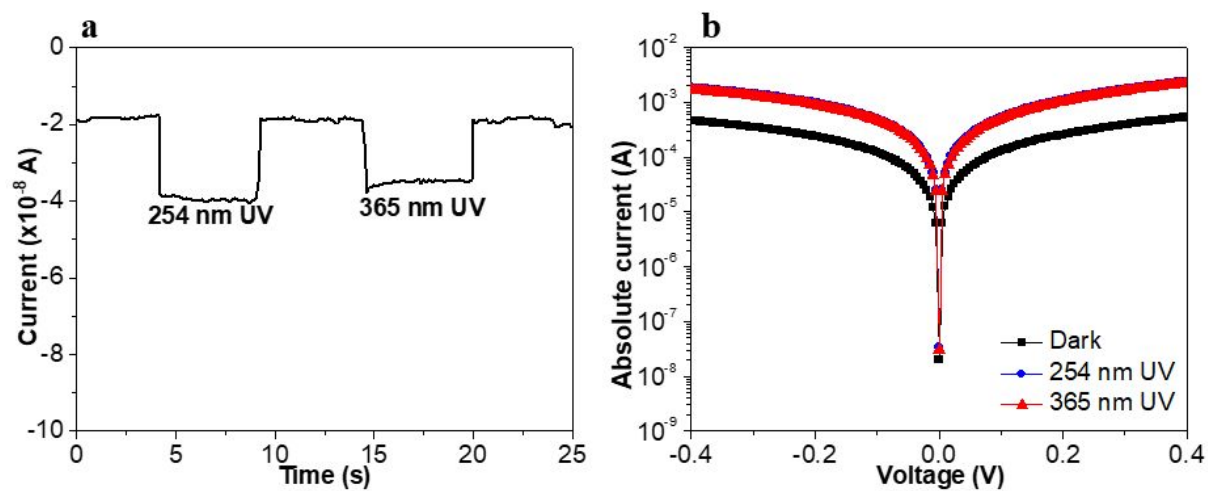


**Figure S7.** Photoresponses (a) and I-V plots (b) of the p-n device under 254 nm- and 365 nm- UV illumination at 0 V.

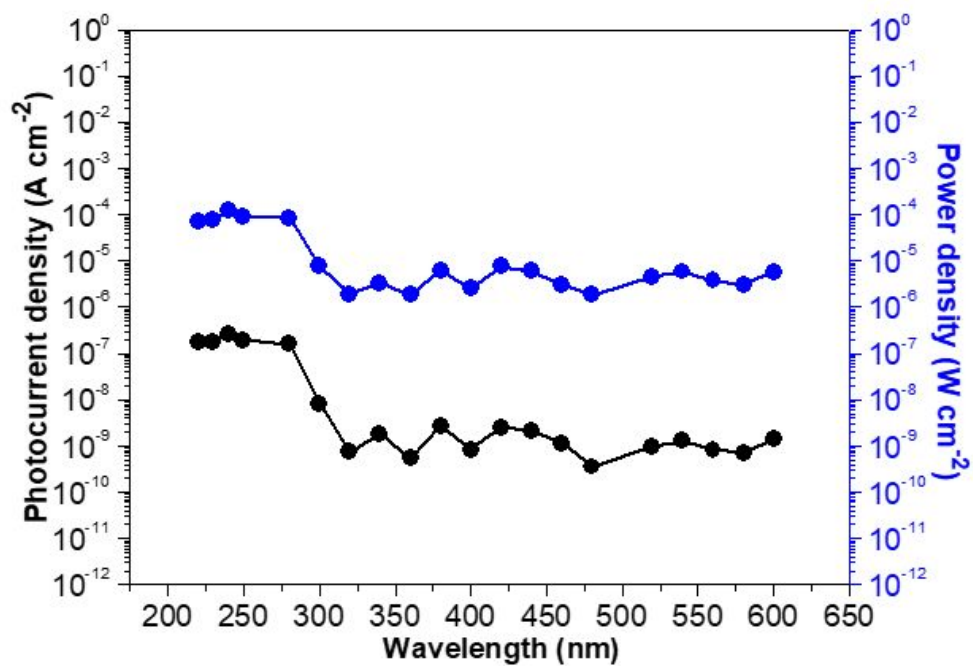


**Figure S8.** Photocurrent density of  $\text{pi}_2\text{n}$  device at 0 V and power density of light source with wavelength in the range of 220-600 nm.

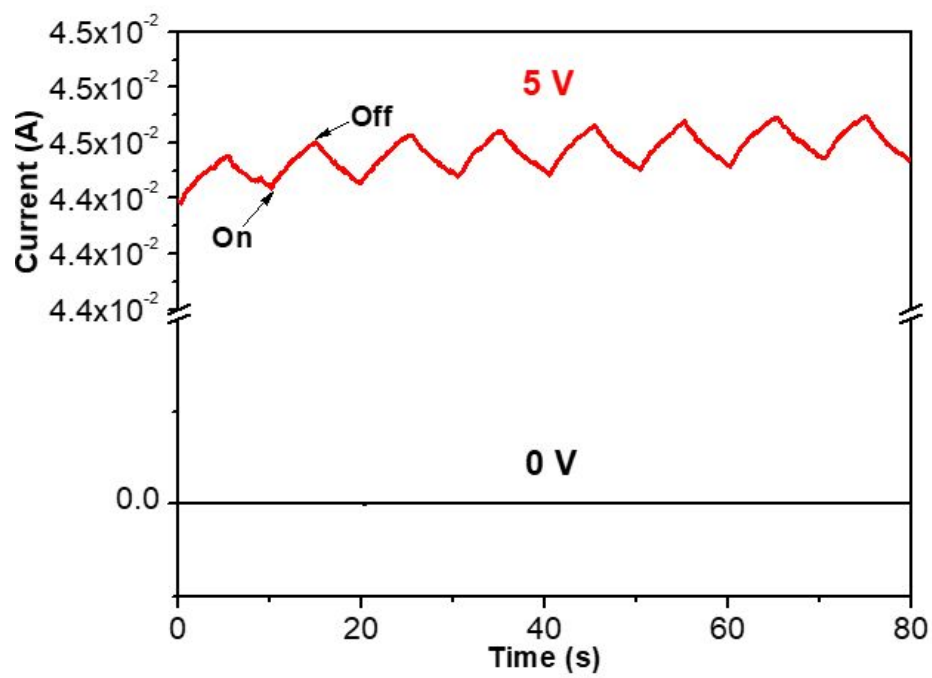


**Figure S9.** Photoresponse of  $\text{CaSnO}_3$ -based photodetector with PH1000/ $\text{CaSnO}_3$ /Ag structure under 254 nm-UV illumination in absence and presence of applied bias (5 V).

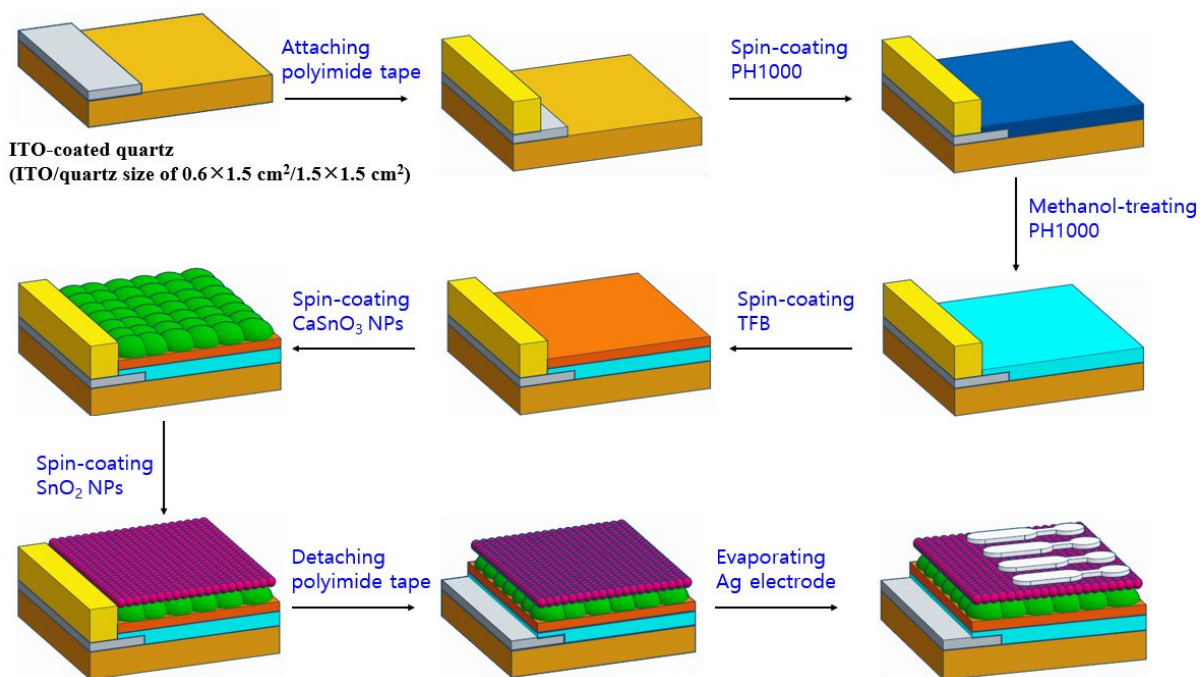


**Figure S10.** Schematic illustration of p-i-n photodetectors preparation.

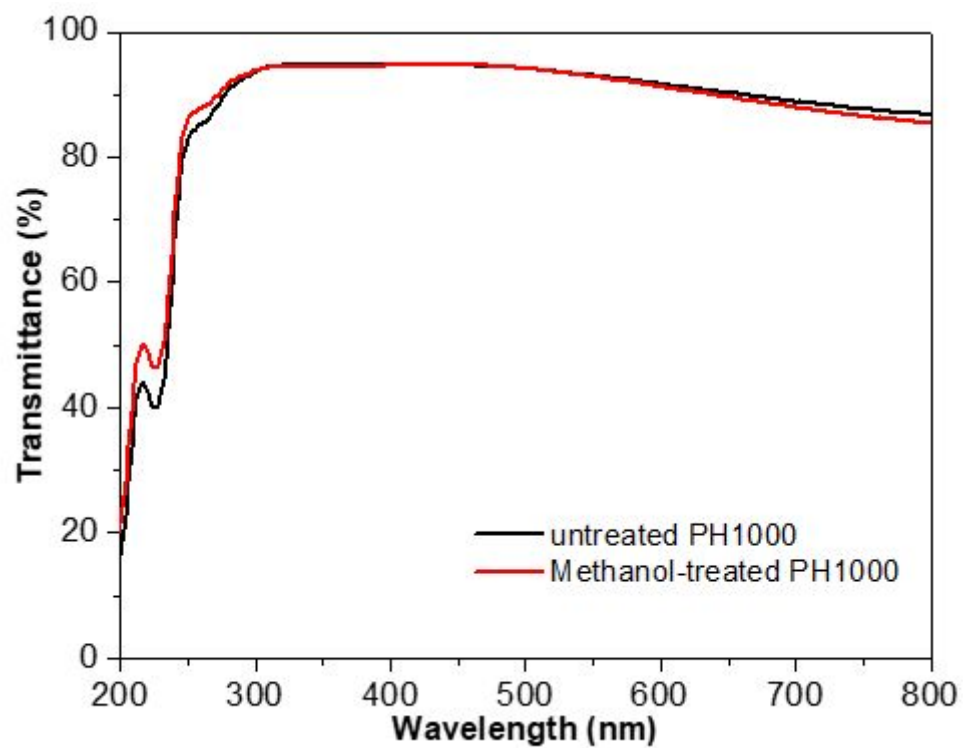


**Figure S11.** UV-Vis spectra of methanol-treated and untreated PH1000 film.